Open access • Journal Article • DOI:10.1617/S11527-014-0308-5

Effect of ionic crosslinking on the swelling and mechanical response of model superabsorbent polymer hydrogels for internally cured concrete — Source link

Qian Zhu, Christopher W. Barney, Kendra A. Erk

Institutions: Purdue University

Published on: 01 Jul 2015 - Materials and Structures (Springer Netherlands)

Topics: Self-healing hydrogels, Superabsorbent polymer, Swelling capacity and Swelling

4-8-2014

Effect of Ionic Crosslinking on The Swelling and Mechanical Response of Model Superabsorbent Polymer Hydrogels for Internally Cured Concrete

Qian Zhu

Christopher W. Barney

Kendra Erk

Effect of ionic crosslinking on the swelling and mechanical response of model superabsorbent polymer hydrogels for internally cured concrete

Qian Zhu, Christopher W. Barney, and Kendra A. Erk*

School of Materials Engineering, Purdue University, 701 West Stadium Avenue, West Lafayette, IN, 47907 USA

*corresponding author: erk@purdue.edu, 1-765-494-4118

Abstract

The chemical and physical structure-property relationships of model superabsorbent polymer (SAP) hydrogels were characterized with respect to swelling behavior and mechanical properties in different ionic solutions (Na^+, Ca^{2+}, and Al^{3+}). The model hydrogels were composed of poly(sodium acrylate-acrylamide) (PANa-PAM) copolymer with varying concentrations of PANa (0, 17, 33, 67, and 83 wt.%) and covalent crosslinking densities of 1, 1.5, and 2 wt.%. By synthesizing the hydrogels in-house, systems with independently tunable amounts of covalent crosslinking and anionic functional groups were created, allowing for the relative effects of covalent and ionic crosslinking on the properties of the hydrogels to be directly quantified. It was found that the presence of Ca^{2+} and Al^{3+} in the absorbed fluid significantly decreased the swelling capacity and altered the swelling kinetics of the PANa-PAM hydrogels. The presence of Al^{3+} in solution resulted in the unexpected formation of a mechanically stiff barrier layer at the hydrogel's surface, which hindered the release of fluid and caused the overall elastic modulus of the hydrogel to increase from *O*(10 kPa) for hydrogels immersed in Ca^{2+} solutions to *O*(100 kPa) for hydrogels immersed in Al^{3+} solutions. Tensile tests performed on isolated specimens of the stiff barrier layer yielded elastic moduli in the *O*(50-100 MPa) range.

Keywords: superabsorbent polymers (SAP), cement hydration, high-performance concrete, multi-valent ions, swelling kinetics

1.0 Introduction

High Performance Concrete (HPC) has increased strength and denser microstructures than ordinary concrete due to lower water/cement ratios and the addition of silica fume.(Breitenbiicher

1998) However, the major limitation of HPC is the occurrence of autogenous shrinkage in the early stages of curing which can lead to cracking and compromised strength.(Weiss et al. 1998) This occurs because the internal relative humidity of HPC decreases dramatically during the hydration process, and without an extra source of water, self-desiccation commonly results and compressive stresses build up which ultimately causes autogenous shrinkage. (Jensen and Hansen 2001; Lura et al. 2003)

Internal curing is considered to be an effective method to reduce self-desiccation. By incorporation of materials with high water storage capacity, referred to as internal curing agents, the stored water can be released into the concrete matrix during the curing process in order to mitigate self-desiccation.(Geiker et al. 2004) Internal curing has been examined by researchers for nearly fifteen years(Kovler and Jensen 2007) and has recently begun to be implemented on bridges in New York,(Di Bella et al. 2012b; Streeter et al. 2012) Indiana,(Schlitter et al. 2010; Di Bella et al. 2012a) and Utah.(Guthrie and Yaede 2013)

Lightweight aggregate (LWA) is one class of internal curing agents and has been found to be very effective at reducing or eliminating autogenous shrinkage.(Bentur et al. 2001; Cusson and Hoogeveen 2008) Yet incorporation of LWA can compromise the final compressive strength of concrete through the formation of voids and flaws in the cured cement that display a range of sizes and morphology.(Bentz and Halleck 2006) Another widely studied class of internal curing agents is superabsorbent polymers (SAPs). SAP hydrogel particles can increase in volume or "swell" up to 1,000 times their original weight when in the presence of water.(Lura et al. 2012) When added to concrete mixtures, SAP particles provide a continuous supply of water during curing, thus reducing/eliminating autogenous shrinkage and cracking of the cement and achieving a corresponding increase in compressive strength and durability.(Jensen and Hansen 2001; Siramanont et al. 2010; Schlitter et al. 2013) Though many of the benefits of incorporating SAPs into cement have been defined in the past, research is still uncovering additional benefits, such as the ability of SAP particles to enhance the freeze/thaw resistance of cement,(Reinhardt et al. 2008; Hasholt et al. 2012; Jones 2013) to reduce thermal expansion,(Wyrzykowski and Lura 2013) or to heal cracks.(Snoeck et al. 2012)

SAP particles are polymer hydrogels composed of polyelectrolyte (charged polymer) chains which are covalently crosslinked to form a three-dimensional polymer network. Driven by osmotic pressure, dry SAP particles swell when in contact with an aqueous fluid(see Figure 1).(Buchholz 1998)

Osmotic pressure results from the formation of a chemical potential gradient in the system due to the relatively high concentration of ions within the SAP's polymer network compared to the external environment. The most common SAP hydrogels used for internal curing are composed of covalently crosslinked poly(acrylic acid-acrylamide) molecules.(Staples et al. 1998) The carboxylic acid groups of the acrylic acid monomer will deprotonate at pH > 5 (forming an anionic moiety, COO^- in Figure 1), whereas the amide groups of the acrylamide monomer are partially hydrolyzed to form anionic carboxylic groups along the polymer chain when pH is ~12 or above.(Jar and Wu 1997; Siriwatwechakul et al. 2012) Other times, partially neutralized acrylic acid (*e.g.*, sodium acrylate) is directly used for synthesis, which, when exposed to water, will readily form anionic groups.(Yarimkaya and Basan 2007)

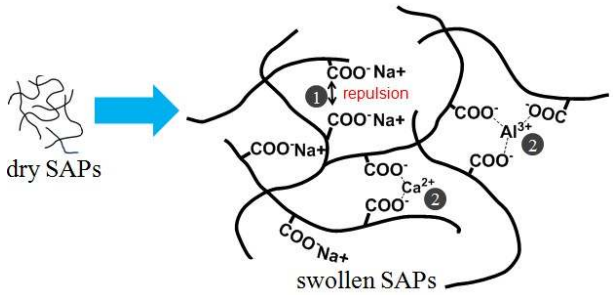

Figure 1. Schematic illustrating the dry and swollen state of a poly(acrylic acid)-based SAP hydrogel particle. Label (1) indicates the electrostatic repulsion force between the anionic carboxylic groups in the polymer network which facilitates swelling. Label (2) indicates potential ionic crosslink formation with multi-valent ions in the fluid which hinders swelling.

In general, there are two polymerization pathways to synthesize SAP particles for internal curing applications: solution polymerization(Chen et al. 2005) and suspension polymerization.(Chen et al. 2004) Crushed SAP particles made from solution polymerization have irregular shapes while SAP particles made from suspension polymerization are typically regular spheres.(Siriwatwechakul et al. 2010; Esteves 2011) According to Siriwatwechacul, *et al.* (Siriwatwechakul et al. 2012), solution polymerized SAP particles have increased water absorbency because suspension polymerization may form a denser, more tightly crosslinked hydrogel. The covalent crosslinking molecules typically used in acrylic acid-based polymerization are di- and tri-acrylate esters such as ethylene glycol diacrylate (EGDMA).(Buchholz 1994) N,N'-methylene-bis-acrylamide (MBA) is often used as a crosslinking

agent for acrylamide polymerization. Raju, *et al.*(Raju et al. 2003) compared four crosslinking agents – MBA, EGDMA, 1,4-butanediol diacrylate (BDA) and diallyl phthalate (DAP) – for preparation of poly(acrylamide-magnesium methacrylate-potassium acrylate). They found that SAP particles synthesized using MBA as the crosslinking agent had the greatest water absorbency over a range of crosslinking concentrations.

During the hydration process of concrete, multiple ions such as K^+, Na^+, OH^-, and Ca^{2+} are released into the pore solution.(Double et al. 1983) In general, the diffusion of ions into a SAP particle leads to deswelling of the hydrogel because the ions effectively screen the repulsive interactions between charged groups within the polymer network. This screening reduces the driving force of swelling and is illustrated in Figure 1 with Na^+ ions and anionic carboxylic groups in a poly(acrylic acid) polymer network. Calcium ions, Ca^{2+}, have been found to have a particularly strong effect on the overall absorbency and swelling kinetics of SAP particles.(Jar and Wu 1997; Yarimkaya and Basan 2007; Siriwatwechakul et al. 2012) Jar, *et al.*(Jar and Wu 1997) found that divalent cations have stronger interactions with polyacrylamide-based gels than monovalent cations. Recently, Schröfl, *et al.*(Schröfl et al. 2012) showed that the presence of Ca^{2+} in the aqueous fluid will dramatically decrease the absorption capacity and alter the absorption and release kinetics of commercial SAP particles. This ionic interaction ultimately resulted in increased autogenous shrinkage and decreased compressive strength of the final cured cement product. In addition to Ca^{2+}, magnesium ions (Mg^{2+}) have similar effects on the swelling behavior of SAP particles.(Bahaj et al. 2010)

While some research efforts have focused on quantifying the effect of Ca^{2+} on swelling behavior, the exact relationship between ionic sensitivity and the physical and chemical molecular structures of SAP particles has not been directly investigated. In the present work, a series of random poly(sodium acrylate-acrylamide) copolymer (PANa-PAM) hydrogels with systematically varied concentrations of covalent crosslinks and anionic groups within the polymer network were synthesized. The hydrogels were immersed in aqueous fluids containing different ionic concentrations and valency, including Na^+, Ca^{2+}, and Al^{3+} (also a byproduct of cement hydration(Andersson et al. 1989)). The swelling response and mechanical properties of the hydrogels were measured, and the experimental results were related to the physical and chemical structures of the hydrogel.

2.0 Experimental Methods

2.1 Materials

Acrylic acid monomer (AA), acrylamide monomer (AM), N,N'-methylenebisacrylamide crosslinking agent (MBA), sodium metabisulfite ($Na_2S_2O_5$), sodium persulfate ($Na_2S_2O_8$), sodium hydroxide (NaOH), sodium chloride (NaCl), calcium nitrate tetrahydrate ($Ca(NO_3)_2 \cdot 4H_2O$), aluminum sulfate hydrate ($Al_2(SO_4)_3 \cdot H_2O$), Ethylenediaminetetraacetic acid disodium salt concentrate (for 1 L standard solution, 0.1 M EDTA-Na_2), Eriochrome® Black T, magnesium chloride ($MgCl_2$), ammonia buffer solution (pH = 10), methanol were purchased from Sigma-Aldrich and were used as received. Deionized water used in the experiment was produced from a Nanopure® Infinity Barnstead water purification system.

2.2 Synthesis of PANa-PAM Hydrogels

Poly(sodium acrylate-acrylamide) (PANa-PAM) was synthesized through free radical solution polymerization of 100 wt.% neutralized acrylic acid and acrylamide monomer according to Horkay*, et al.*(see Figure 2).(Horkay et al. 2000)(Horkay et al. 2001) As acrylic acid is neutralized before polymerization, this will result in a polymer network in which the anionic groups are from the acrylic acid segments of the chain (*i.e.*, COO^-) and the acrylamide segments remain intact and subsequently un-charged. NaOH was used to neutralize the acrylic acid monomer prior to synthesis. Redox initiator solution was obtained by separately dissolving $Na_2S_2O_5$ and $Na_2S_2O_8$ in deionized water to concentrations of 0.5 wt.%. Aqueous solutions of MBA were used for crosslinking. These solutions were prepared 1 day in advance to allow MBA powder to dissolve fully. The covalent crosslinking densities used in present work were 1.0 wt.%, 1.5 wt.% and 2.0 wt.% (by monomer weight) and initiator concentration was 1 wt.%. For each selected covalent crosslinking density, the ratio of acrylic acid to acrylamide was varied as: 0 wt.% PANa, 17 wt.% PANa, 33 wt.% PANa, 67 wt.% PANa, 83 wt.% PANa.

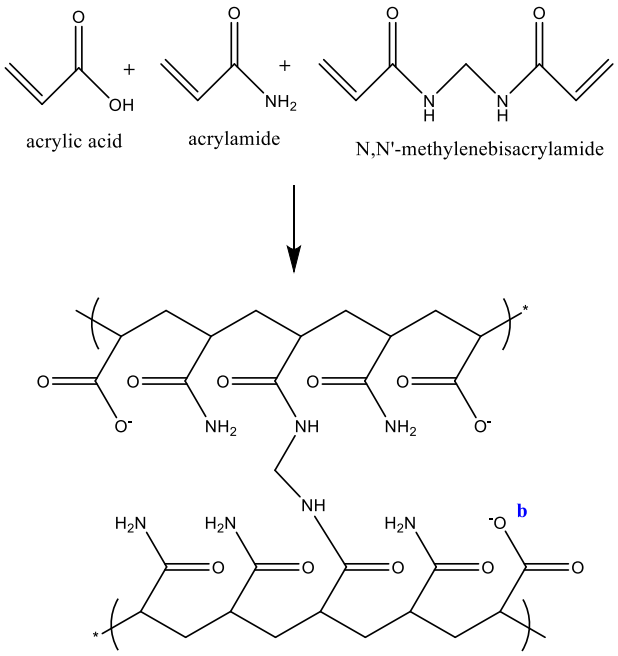

Figure 2. Reaction scheme of PANa-PAM hydrogel synthesis. The polymer network of the hydrogel contains covalent crosslinks (a) and anionic carboxylate groups (b).

To perform the synthesis, the initiator solution was added to a mixture of neutralized acrylic acid, acrylamide, and crosslinking agent and stirred. An exothermic reaction began within a few seconds for the pure acrylamide system (*i.e.*, 0 wt.% PANa). The reaction occurred rapidly (few minutes) and a clear hydrogel was observed to form. For other PANa-PAM ratios, the formation time varied from a few minutes to few hours. All vials were allowed to rest for another 24 hours, at least, after the gel formation to ensure reaction completion. To obtain the hydrogel, the glass vial was crushed. All the hydrogel samples were elastic and thus retained the cylindrical shape of the vial. Hydrogel samples were washed with water and crushed to form smaller pieces, which were then dried overnight at 80℃. Dried PANa-PAM particles were then ground further into fine particles (using a mortar and pestle). Using a series of sieves, two final (dry) particle size distributions were obtained: 106-425 μm and 425-850 μm. Another set of hydrogels were cut into quarters followed by drying overnight at 80℃ for macroscale swelling studys and mechanical testing.

2.3 Swelling Measurements of Hydrogels

The gravimetric “teabag” method was used to evaluate the overall swelling capacity and kinetics of the PANa-PAM hydrogel samples.(Yarimkaya and Basan 2007; Zhang et al. 2010) Four different

immersion solutions were studied: pure deionized water, 0.025 M Na^+ (from NaCl), 0.025 M Ca^{2+} (from $Ca(NO_3)_2 \cdot 4H_2O$), and 0.025 M Al^{3+} (from $Al_2(SO_4)_3 \cdot H_2O$).

The measurement procedure was as follows: 0.2 g dry sample were added into a pre-wetted teabag and immersed in 200 ml of solution. For 425-850 μm samples, the wet mass was measured after immersion times of 1, 3, 5, 10, 15, 30, 60, 120, and 240 minutes; for 106-425μm samples, the wet mass was measured after immersion times of 30s, 1, 2, 5, 10, 15, 30, 60, and 120 min. The mass was measured after absorbing excess water from the teabag's surface using a paper towel. In this project, bulk PANa-PAM samples (0.35-0.45 g dry, ~8 mm × 8 mm × 5 mm in dimension) were also studied for comparison purposes. For the bulk samples, teabags were not used to assist in the swelling measurement. Immersion volumes of 500 ml were used for these larger samples and the wet mass was tracked for 10 days. For all PANa-PAM samples, the swelling ratio, Q (g/g), was calculated from the following equation:

$$Q = \frac{m_s - m_d}{m_d} \qquad \text{Eq. 1}$$

where m_s was the wet mass of the swollen samples and m_d was the initial dry mass. Samples used for swelling measurements were from different synthesis batches, and measurements were repeated 3 times.

The Ca^{2+} that remained in the immersion solution after the sample reached swelling equilibrium was quantified by basic titration methods.(Gary D. Christian 2004) Calcium ion solutions were titrated by EDTA solution, and Eriochrome® Black T was used as the indicator. Small amounts of Mg-EDTA solution was added to calcium ion solution for a sharper color change, from wine red through purple to a pure blue, at the end point.

2.4 Mechanical Characterization of Hydrogels

PANa-PAM hydrogel samples that were swollen in Ca^{2+} solutions were tested in compression by dynamic mechanical analysis (DMAQ800, TA Instruments) to obtain the stress response as a function of strain for each sample. The mode was "force control", preload force was 0.1 N, and the force ramp was 0.2 N/min. The samples were cut into 6-mm×6-mm×4-mm cubes for compression testing.

PANa-PAM hydrogel samples swollen in Al^{3+} solutions did not display isotropic properties (as described in the results section) and could not be cut into the smaller samples that were required for

testing with the DMA. Therefore, these samples were tested under compression mode with an MTS mechanical testing load frame with compression platens. Samples were roughly 1/4 of a round disc with diameter of 20mm and thickness of 10mm The preload force was 1 N and load rate was 1 mm/min. Data was collected regardless of the unusual sample shape in order to have an overall evaluation of the sample's mechanical properties. In the future, more regular disc shapes will be synthesized. Rectangular strips (5-mm×3-mm×0.5-mm) of the stiff outer region of the PANa-PAM hydrogel samples swollen in Al^{3+} solutions were tested in tension with the DMA.

3.0 Results and Discussion

3.1 Swelling Behavior of PANa-PAM Hydrogel Samples in Water and Na^+ Solutions

Figure 3 and 4 displays the transient swelling ratio for PANa-PAM hydrogel samples containing different concentrations of PANa in deionized water and Na^+ solutions. After a quick initial intake of water at short times, the swelling ratio reached an effective plateau within approximately 50 minutes for all the hydrogel samples. In general, the maximum swelling ratio and the initial swelling rate were observed to increase for hydrogels that contained greater concentrations of PANa in the polymer network. For example, for a hydrogel sample with 2 wt.% covalent crosslinking density, the initial swelling rate in Na^+ solution was 3.7 $(g/g)min^{-1}$ for the 17 wt.% PANa sample and increased to 24.3 $(g/g)min^{-1}$ for the 83 wt.% PANa sample (note: both rates were calculated for the first 5 min of immersion).

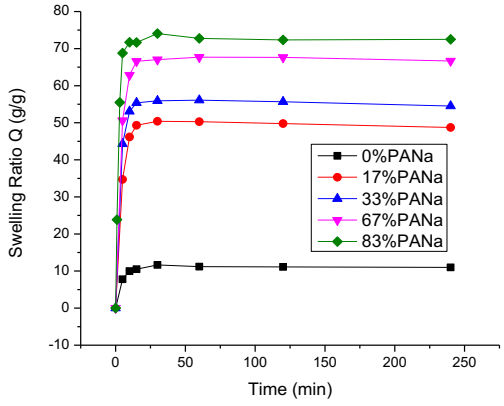

Figure 3. Absorption of 425-850μm PANa-PAM hydrogel samples with 2 wt.% covalent crosslinking density in deionized water.

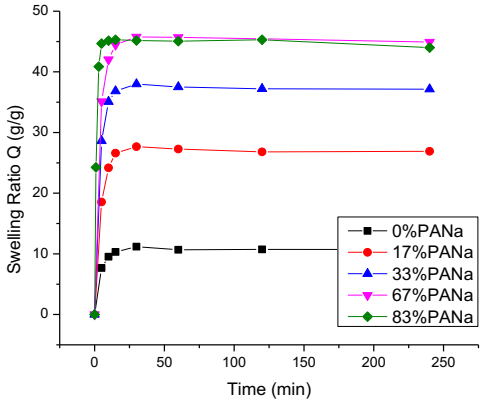

Figure 4. Absorption of 425-850μm PANa-PAM hydrogel samples with 2 wt.% covalent crosslinking density in Na^+ solution.

The final swelling ratio at long times (*e.g.*, ~ 4h) was known as the equilibrium swelling ratio and is reported in Table 1 for PANa-PAM hydrogel samples containing different covalent crosslinking densities and PANa concentrations. For all the samples, the equilibrium swelling ratio obtained from immersion in Na^+ solutions was reduced compared to the swelling ratio in deionized water. Consistent with Figure 3 and 4, PANa-PAM hydrogel samples that contained greater concentrations of PANa in its polymer network displayed a correspondingly increased equilibrium swelling ratio from immersion in water and Na^+ except for one abnormal point (H_2O, 33 wt% PANa, 1% crosslinking density). This odd point might result from imperfection of synthesis. More controlled synthesis methods will be investigated in the future.

Table 1 also indicates that increased covalent crosslinking density led to decreased swelling ratio for samples immersed in deionized water or Na^+ solutions. For 17 wt.% PANa sample, the swelling ratio decreased from 105.1 g/g to 41.7 g/g (in water) and from 43.3 g/g to 23.3 g/g (in Na^+ solution) as the covalent crosslinking density increased from 1 wt.% to 2 wt.%. This trend is consistent with published results; for example, the swelling ratio of poly(acrylamide-co-sodium methacrylate) decreased from 250g/g to140g/g as the concentration of crosslinking agent increased from 0.016 mM to 0.032 mM.(Murali Mohan et al. 2006)

Table 1. Equilibrium (long-time) swelling ratios, *Q* (g/g), of 425-850 μm PANa-PAM hydrogel samples immersed in pure deionized water, 0.025 M Na^+, 0.025 M Ca^{2+}, and 0.025 M Al^{3+} solutions. Whenever possible, averages and 1 standard deviation are reported in the table (n = 3-4).

		PANa Concentration (in polymer network)				
Covalent Crosslinking	**Solution**	**0 wt.%**	**17 wt.%**	**33 wt.%**	**67 wt.%**	**83 wt.%**
1.0 wt.%	H_2O	14.9	105.1 ± 7.9	89 ± 24.9	116.1 ± 5.9	125.0 ± 3.9
	Na^+	14.3	43.3 ± 3.0	47.5 ± 11.1	60.5 ± 3.1	62.7 ± 6.1
	Ca^{2+}	14.1	11.1 ± 2.7	10.6 ± 5.1	2.9 ± 0.4	1.9 ± 0.3
	Al^{3+}	13.4	3.4 ± 0.1	2.6 ± 0.3	8.6 ± 3.2	13.3 ± 7.0
1.5 wt.%	H_2O	13.9	65 ± 12.5	67.6 ± 26.5	90 ± 15.4	113.4 ± 20.6
	Na^+	13.2	32.5 ± 3.1	41.6 ± 14.4	53.3 ± 6.5	59.8 ± 6.8
	Ca^{2+}	11.4	11.7 ± 1.8	6.8 ± 0.2	3.0 ± 1.5	1.9 ± 0.5
	Al^{3+}	11.5	2.8 ± 0.8	2.4 ± 0.4	5.3 ± 1.0	7.1 ± 2.3
2.0 wt.%	H_2O	11.0	41.7 ± 13.8	50 ± 7.9	68.2 ± 6.5	74.3 ± 8.3
	Na^+	10.7	23.3 ± 4.7	33.2 ± 4.6	41.3 ± 4.2	44.8 ± 3.2
	Ca^{2+}	10.8	8.2 ± 1.4	7.1 ± 0.4	2.7 ± 0.5	2.2 ± 0.1
	Al^{3+}	9.4	2.9 ± 1.0	2.6 ± 0.7	3.3 ± 2.2	8.7 ± 5.4

The swelling behavior of hydrogel samples in solutions containing different ion concentrations was also investigated (Figure 5). As shown in Figure 5a, the equilibrium swelling ratio of a representative hydrogel sample decreased as the Na^+ ion concentration of the swelling solution increased from 0.0125 M to 0.1 M. The swelling rate also decreased as ion concentration increased (shown in Figure 5b). For example, the hydrogel sample immersed in 0.0125 M solution increased to 61 g/g within the first 5 minutes while the sample immersed in 0.1 M solution only reached 30 g/g.

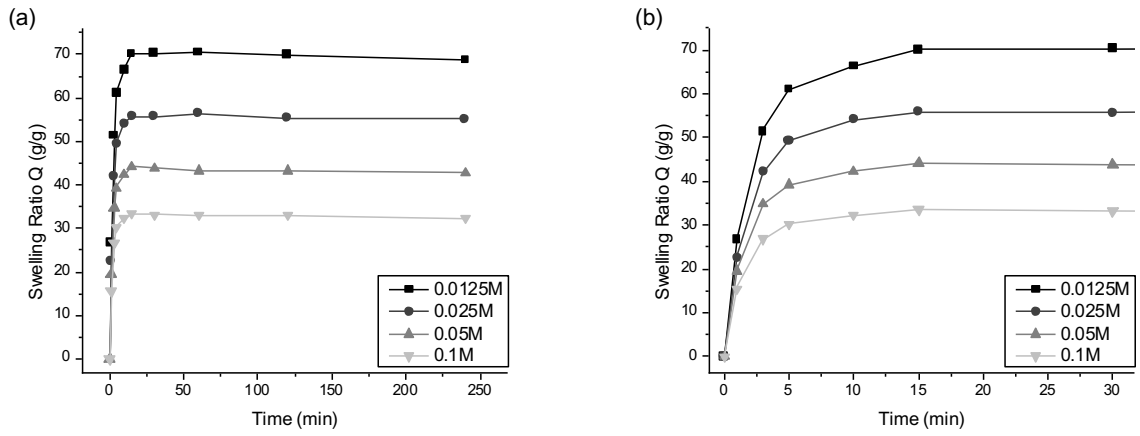

Figure 5. Swelling behavior of 425-850μm 33 wt.% PANa, 1 wt.% covalently crosslinked PANa-PAM hydrogel sample immersed in Na^+ solutions with varying ion concentrations over the full immersion time of 240 min (a) and during the first 30 min of immersion (b).

Discussion

The driving force for swelling (*i.e.*, osmotic pressure) was related to the ion concentration difference internal and external to the hydrogel sample, referred to here as the ion concentration gradient. In the PANa-PAM hydrogels that were studied, the concentration of anionic groups within the hydrogel was directly proportional to the amount of PANa within the polymer network, which varied according to the selected monomer feedstock ratio used for the hydrogel synthesis. Thus, the PANa-PAM hydrogel samples with higher PANa concentrations had greater internal ion concentrations which explains the increased swelling ratios reported in Table 1 when immersed in the same swelling media (deionized water or 0.025 M Na^+). Likewise, the swelling ratio of a given PANa-PAM hydrogel sample directly depends upon the ion concentration of the immersion solution. From Table 1, the equilibrium swelling ratio was higher for all the PANa-PAM hydrogel samples immersed in deionized water (larger ion concentration gradient) than in Na^+ solutions (smaller ion concentration gradient). The relationship was further confirmed by immersing samples in Na^+ solutions with different ion concentrations (Figure 5). Swelling was reduced for PANa-PAM hydrogels immersed in solutions containing higher concentrations of Na^+.

According to rubber elasticity theory(Rubinstein and Colby 2003), the elastic shear modulus, G, of a crosslinked polymer network is related to the molecular weight of the polymer chain between neighboring crosslinks. The equation to describe this is as follows:

$$G \approx \frac{nkT}{V} \approx \frac{\rho RT}{Ms} \qquad \text{Eq. 2}$$

where n / V is the number of elastically active network strands per unit volume, k is the Boltzmann constant, T is the temperature, R is the gas constant, ρ is the mass per unit volume (*i.e.*, the network density), and M_S is the average molecular weight of between two crosslink points. Thus, the elastic shear modulus of a crosslinked hydrogel will increase as the concentration of crosslinks in the network increases.(Henderson et al. 2010) During the swelling process for PANa-PAM hydrogels, an equilibrium is reached between elongation force which comes from osmotic pressure and the retraction force which originates from the network's elastic shear modulus.(Buchholz 1998) Thus, as covalent crosslinking density increased in the PANa-PAM hydrogel samples, the elastic shear modulus increased which led to larger retraction forces within the network and a corresponding decrease in swelling ratio (see Table 1). Experiments were performed to measure the mechanical properties of the hydrogel samples and these are described in Section 3.5.

3.2 Swelling Behavior of PANa-PAM Hydrogels in Ca^{2+} and Al^{3+}Solutions

Figure 6 and 7 displays the swelling behavior for hydrogel samples with different PANa concentrations immersed in Ca^{2+} and Al^{3+} solutions. In Ca^{2+} solutions, the equilibrium swelling ratios decreased as PANa concentrations increased (Figure 6, average values reported in Table 1). For example, for a hydrogel sample from Table 1 with 2 wt.% covalent crosslinking density immersed in Ca^{2+} solutions, the swelling ratio decreased from 10.8 g/g to 2.2 g/g as the PANa concentration increased from 17 wt.% to 83 wt.%. In Al^{3+} solutions, the equilibrium swelling ratios decreased and then increased as PANa concentrations increased (Figure 7, average values reported in Table 1). For 17 wt.% and 33 wt.% PANa concentration samples, the swelling ratio in Ca^{2+} solutions was larger than in Al^{3+} solutions while for 67 wt.% and 83 wt.% PANa concentration samples, the swelling ratio in Ca^{2+} solutions was smaller than in Al^{3+} solutions.

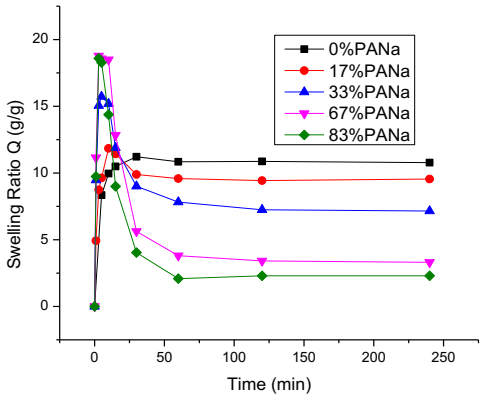

Figure 6. Absorption of 425-850μm PANa-PAM hydrogels with 2 wt.% covalent crosslinking density in Ca^{2+} solution.

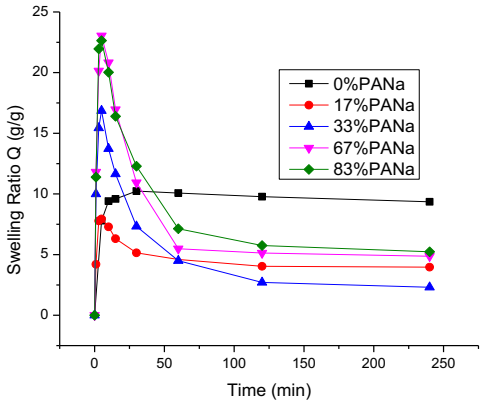

Figure 7. Absorption of 425-850μm PANa-PAM hydrogels with 2 wt.% covalent crosslinking density in Al^{3+} solution.

As shown in Table 1, the equilibrium swelling ratios of hydrogels immersed in Ca^{2+} and Al^{3+} solutions were significantly reduced compared to the ratios of samples swollen in water and Na^{+}. For example, the swelling ratio of a 33 wt.% PANa, 2 wt% crosslinking density sample decreased from 33.2 g/g in Na^{+} solution to 7.1 g/g in Ca^{2+} solution and 2.6 g/g in Al^{3+} solution. Compared with the swelling behavior of samples immersed in deionized water or Na^{+} solutions, the covalent crosslinking density did not have a significant effect on the samples immersed in Ca^{2+} or Al^{3+} solutions (see Table 1). For example, the swelling ratio for 67 wt.% PANa concentration samples was around 3.0 g/g (immersed in Ca^{2+} solutions) for 1, 1.5, or 2 wt.% covalent crosslinking density. Additionally, the samples immersed in Al^{3+} solutions appeared to become much stiffer (mechanically) compared with other samples.

The swelling kinetics were also observed to change when hydrogel samples were immersed in Ca^{2+} and Al^{3+} solutions compared with the behavior observed during immersion in pure water or Na^{+} solutions. At short immersion times, an obvious peak was observed for samples containing PANa in the polymer network while no significant peak was observed for the 0 wt.% PANa sample (*i.e.*, 100 wt.% PAM). The peaks in the swelling responses indicated a rapid swelling of the hydrogel sample immediately followed by a de-swelling or release of fluid from the sample. In both Figure 6 and 7, hydrogel samples containing a majority concentration of PANa attained the greatest short-time swelling ratios (*i.e.*, displayed the highest peaks). Additionally, the peaks for samples immersed in Ca^{2+} solution became narrower as PANa concentration increased (Figure 6) while the peaks became broader as PANa concentration increased for samples immersed in Al^{3+} solution (Figure 7). Similar to results in Section 3.1, the initial swelling rate increased as PANa concentration increased but the trend was much weaker. For example, for a hydrogel sample with 2 wt.% covalent crosslinking density, the initial swelling rate in Ca^{2+} solution was 3.0 $(g/g)min^{-1}$ for the 17 wt.% PANa sample and increased to 3.8 $(g/g)min^{-1}$ for the 83 wt.% PANa sample (note: both rates were calculated for the first 5 min of immersion).

To determine the amount of Ca^{2+} ions absorbed by the hydrogel samples, titration was performed on the immersion solution remaining after a hydrogel sample was allowed to swell and reach equilibrium in Ca^{2+} solution for 4 h. The amount of Ca^{2+} absorbed by each sample was calculated by subtracting the amount of Ca^{2+} consumed by titration from the initial Ca^{2+} added in the swelling media (*i.e.*, 0.025M). Figure 8 shows the concentration of absorbed Ca^{2+} ions as a function of PANa concentration in the polymer network of the hydrogel sample. Greater concentrations of Ca^{2+} ions were absorbed by polymer networks containing greater PANa concentrations.

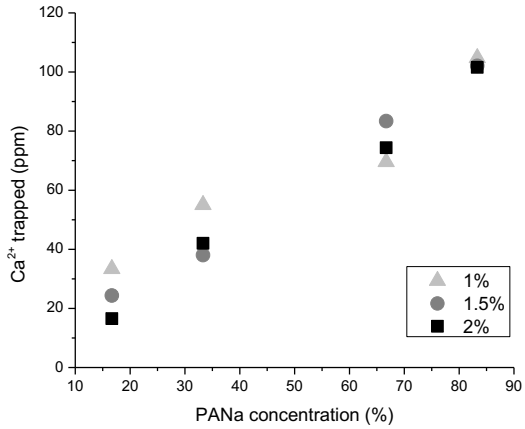

Figure 8. The concentration of Ca^{2+} trapped by 425-850μm PANa-PAM hydrogels with 1 wt.%, 1.5 wt.%, 2 wt.% crosslinking density after 4 h immersion time (as determined by titration).

Discussion

As observed in Figures 6 and 7, the overall absorption capacity and swelling kinetics of PANA-PAM hydrogel samples immersed in multi-valent Ca^{2+} or Al^{3+} solutions were dramatically different compared with hydrogel samples swollen in pure water or Na+ solutions. The equilibrium swelling ratio decreased for hydrogels immersed in the multi-valent solutions, and the reduction was strongest for hydrogels containing greater concentrations of PANa in the polymer network. Swelling kinetics of the hydrogels immersed in the multi-valent solutions displayed fast swelling immediately followed by fast fluid release. Additionally, post-swelling titration analysis displayed in Figure 8 indicated that the largest concentrations of Ca^{2+} ions were trapped by the hydrogel samples containing the greatest concentrations of PANa.

The reduced PANa-PAM hydrogel swelling in Ca^{2+} and Al^{3+} solutions compared with those swollen in water or Na^{+} solutions is believed to be due to the diffusion of Ca^{2+} or Al^{3+} ions into the hydrogel network and the subsequent formation of complexes or "ionic crosslinks" with the anionic groups in the polymer network (derived from incorporation of PANa into the network). This explanation is consistent with the results shown in Figure 6, 7 and 8, illustrating that PANa-PAM hydrogel samples which contained a greater concentration of PANa were more sensitive to the presence of multi-valent ions, displaying greater reductions in swelling and a greater absorption of Ca^{2+}. It is inferred that polymer networks within the PANa-PAM hydrogel samples were more

sensitive to trivalent ions (Al^{3+}) than divalent ions (Ca^{2+}) due to the fact that the samples containing 17 and 33 wt.% PANa have a more reduced equilibrium swelling ratio in Al^{3+} solutions than in Ca^{2+} solutions (note: the reverse is true for samples contianing >33 wt.% PANa and this is explained in Section 3.4 and 3.5). Additionally, ionic crosslinking propensity had a much stronger impact on swelling behavior than the concentration of covalent crosslinks even for samples with small amounts of PANa.

Additionally, the observed change in swelling kinetics due to the presence of multi-valent ions was most likely related to the time-dependent formation of ionic crosslinks within the polymer network of the hydrogel. At short immersion times, PANa-PAM hydrogel samples containing relatively high concentrations of PANa displayed greater overall absorption and faster swelling rates due to the correspondingly large ion concentration gradient driving the swelling response. However, as the ions diffuse over time and form ionic crosslinks, samples containing a greater concentration of PANa formed a proportionally greater concentration of ionic crosslinks within the polymer network, leading to a large reduction in swelling and the formation of the swelling peaks in Figures 6 and 7. This internal competition between swelling due to ion concentration gradients and deswelling from ionic crosslinking explains why in Figure 6 and 7 the maximum value of the short-term swelling ratio peak approaches a limiting value even though the concentration of PANa in the polymer network continued to increase (*e.g.*, from 67 wt.% to 83 wt.%).

The overall reduction of swelling due to the presence of ionic crosslinks between multi-valent ions and the polymer network of the hydrogel samples is most likely due to a combination of (1) physical restriction of the polymer chains (*i.e.*, decreased extensibility) due to the formation of physical crosslinks between neighboring chain segments and (2) a change in the chemical potential of the hydrogel due to the decreased ion concentration. A single Ca^{2+} ion is expected to form complexes with 2 COO^- groups while a single Al^{3+} ion can form complexes with 3 COO^- groups. Prior work by Horkay, *et al.*,(Horkay et al. 2000) has found that Ca^{2+} ions were delocalized within the polymer networks of swollen hydrogels and were believed to promote aggregation of individual polymer chain segments into loose bundles. This aggregation may restrict the motion of the polymer segments somewhat but was observed to not directly affect the elastic modulus of the hydrogel; any change in the elastic modulus was only a function of the degree of swelling.(Horkay et al. 2000) Thus, the ionic crosslinks formed by Ca^{2+} are considered to be relatively weak physical crosslinks. It is expected that

stronger, localized ionic crosslinks are formed between trivalent Al^{3+} and anionic groups in the polymer network, as previous work has shown that rare earth cations (La^{3+} and Ce^{3+}) bind irreversibly to polyacrylate polymer network, causing permanent de-swelling of the hydrogels.(Horkay et al. 2001) The implications of these "weak" Ca^{2+} and "strong" Al^{3+} ionic crosslinks in the PANa-PAM hydrogel samples will be explored further in Section 3.5 with characterization of the samples' mechanical properties.

3.3 Effect of PANa-PAM Hydrogel Sample Size

In all previously described results, PANa-PAM hydrogel samples were composed of particles of size 425-850 μm. To determine the effect of the chosen size range on the swelling behavior and ionic sensitivity, hydrogel samples composed of 106-425 μm particles were created and characterized. Both particle size ranges are compared in Figure 9, which displays the swelling curves for 17 wt.% and 83 wt.% PANa concentration PANa-PAM hydrogel samples in pure water and Ca^{2+} solutions. The measured equilibrium swelling ratios were found to be independent of particle size. As expected, the swelling rate was faster for the smaller hydrogel particles. It required 2 minutes for the 106-425 μm particles to reach its maximum swelling ratio but approximately 10-15 minutes for the 425-850 μm particles to reach their maximum swelling ratio.

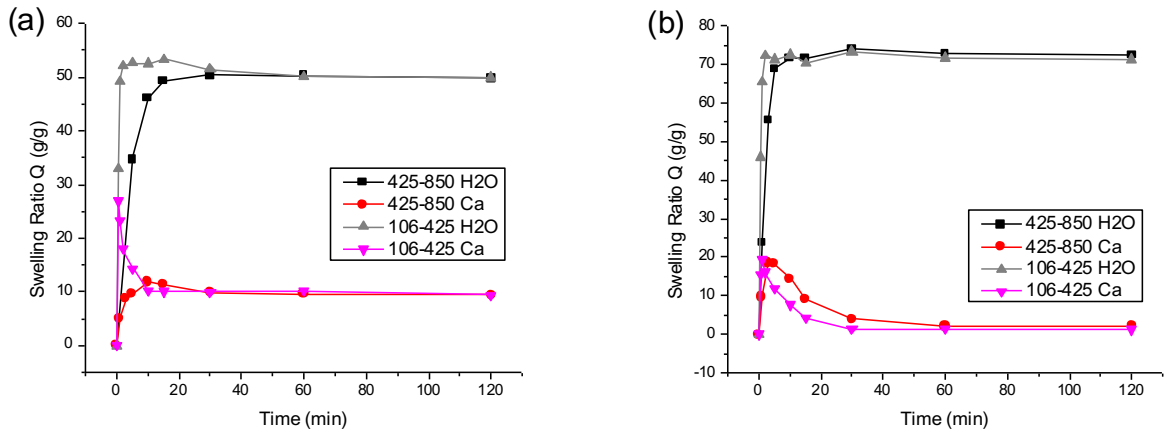

Figure 9. The transient swelling response as a function of sample size (106-425 μm, 425-850 μm) and immersion solution (pure water, Ca^{2+}) for two different hydrogel compositions: (a) 17 wt.% PANa-PAM hydrogel sample, 2 wt.% covalent crosslinking density and (b) 83 wt.% PANa-PAM hydrogel sample, 2 wt.% covalent crosslinking density.

Discussion

The size of SAP particles has important implications for the real-world application in cement. Jensen and Hansen(Jensen and Hansen 2002) showed that small SAP particles (a few μm across) may show a decreased absorbency due to less active surface zone compared to the bulk. The simulation results indicated that particle size about 100-200 μm was efficient for water diffusion in cement paste. But in the present study, no significant absorbency difference was observed for the two investigated particle size ranges, most likely because the two selected size ranges relatively large (> 100 μm) such that no significant absorbency difference was observed.

As shown in Figure 9, the particle size had a very strong effect on the swelling kinetics of the samples. The observed increase in swelling rate as particle size decreased is consistent with results from Esteves.(Esteves 2011) The author studied 50-500 μm SAP particles swollen in synthetic pore solution with optical microscopy. As swelling is controlled by diffusion of fluid into the hydrogel, the size dependence can be described by Fick's second law, as given by the following equation:

$$\frac{dQ}{dt} = k(Q_{max} - Q) \qquad \text{Eq. 3}$$

where Q_{max} and Q are the swelling capacities at equilibrium and at any time t, and k is the swelling rate constant which depends on the particle size and can be described as $k = (2.76 \times 10^3)\ \Phi^{-1567}$ for particles immersed in synthetic pore solution where Φ represents the diameter of the particle (μm).(Esteves 2011) Thus, as particle size decreases, the swelling rate will increase dramatically, consistent with the trends displayed in Figure 9.

3.4 Characterization of Macroscale PANa-PAM Hydrogel Samples

Macroscale (mm-sized) samples of the PANa-PAM hydrogel samples were created and characterized in order to more fully understand the behavior of the hydrogels in multi-valent ion solutions. As described in Section 3.2 (Table 1), the equilibrium swelling ratio of PANa-PAM gels in Al^{3+} solutions was observed to be greater than in Ca^{2+} solutions for the 67 wt.% and 83 wt.% PANa samples, which was not anticipated. Additionally, the samples immersed in Al^{3+} solutions became much stiffer to slight mechanical pressure compared with other samples. To directly quantify the changes in mechanical response, samples with macroscopic dimensions were required in order to use conventional compression testing methods.

Figure 10a displays the transient swelling behavior of macroscale hydrogel samples in Ca^{2+} and Al^{3+} solutions. The equilibrium swelling ratio of 17 wt.% PANa samples in Al^{3+} solutions was smaller than in Ca^{2+} solutions while the equilibrium swelling ratio of 67 wt.% PANa samples in Al^{3+} solutions was greater than results from the Ca^{2+} solutions. This trend is consistent with the swelling behavior of the 425-850μm samples reported in Table 1, though the exact equilibrium values of the macroscale samples differ somewhat. The 17 wt.% PANa sample in Ca^{2+} did not display a peak in the swelling response but did display a broad peak during immersion in the Al^{3+} solution. The 67 wt.% PANa sample displayed narrow peaks in both solutions.

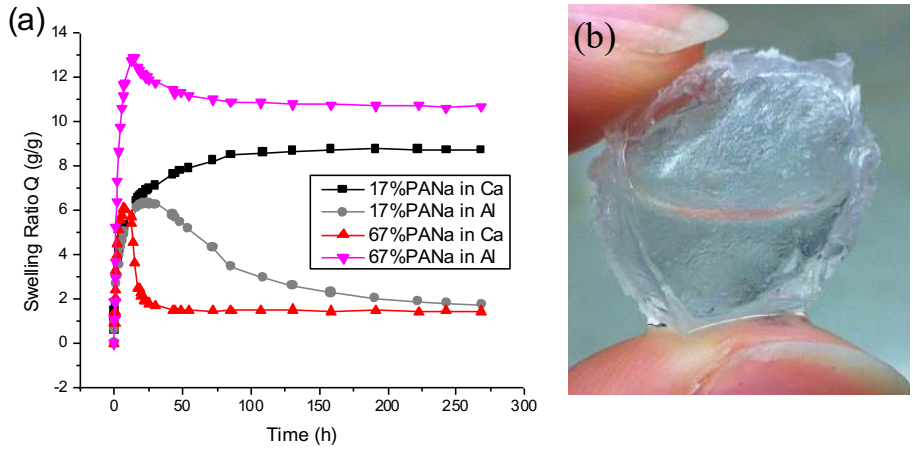

Figure 10. (a) Absorption of macroscale PANa-PAM hydrogel samples with 1 wt.% covalent crosslinking density in Ca^{2+} and Al^{3+} solutions. (b) Photograph of a macroscale PANa-PAM hydrogel sample (67 wt.% PANa, 1 wt.% covalent crosslinking density) following immersion in Al^{3+} solution after reached swelling equilibrium.

The physical characteristics of the macroscale PANa-PAM hydrogel samples swollen to equilibrium in Ca^{2+} or Al^{3+} were very different. The samples immersed in Ca^{2+} solutions appeared to be more elastic and tougher compared to samples immersed in pure water which were easily broken by applying small compressive forces (*e.g.*, by touching with finger). The samples with 17 wt.% PANa concentration immersed in Al^{3+} solutions displayed an even greater increase in elasticity and toughness (behaving more like a hard rubber than a conventional gel) than similar sample immersed in Ca^{2+} solutions. Surprisingly, the 67 wt.% and 83 wt.% PANa hydrogel samples immersed in Al^{3+} solutions formed a stiff, solid-like shell. This shell started to form after 1.5 hours of immersion in the solution. After the PANa-PAM hydrogel sample reached swelling equilibrium, a complete "core-shell" structure formed and was strong enough to successfully retain fluid within the core of the

sample, as shown in Figure 10b. When the sample was carefully sectioned, the fluid-filled core was observed to be mechanically soft and the stiff outer shell could be removed from the sample (note: mechanical tests of the isolated shell are reported in Section 3.5). In the present study, 33 wt.% PANa macroscale samples immersed in Al^{3+} solutions were also studied and this system was not observed for form the core-shell structure.

Discussion

As described in Section 3.2, the formation of ionic crosslinks is believed to lead to a reduction in the equilibrium swelling ratio. This was directly apparent for PANa-PAM hydrogel samples immersed in Ca^{2+} solutions or PANa-PAM hydrogels containing a low concentration of anionic groups (17 wt.% and 33 wt.%) in Al^{3+} solutions.

The main experimental result observed here was the formation of a soft-core/stiff-shell structure of the macroscale hydrogel samples containing >33 wt.% PANa during immersion in Al^{3+} solutions. This core-shell structure directly impacted the swelling response (see Figure 10a) of the hydrogel samples. The stiff shell was believed to be formed by a high density of Al^{3+}-facilitated ionic crosslinks within the outer region of the hydrogel sample. Such an ionic "barrier" appeared to hinder fluid release from the hydrogel sample, explaining the increased equilibrium swelling ratio for 67 wt.% and 83 wt.% PANa samples immersed in Al^{3+} solutions compared with similar samples immersed in the Ca^{2+} solutions (see Figure 10a and Table 1).

It appears that ionic crosslinks formed by divalent ions (Ca^{2+}) only displayed one effect on the equilibrium swelling ratio (*i.e.*, ratio reduction due to network chain retraction), while the ionic crosslinks formed by trivalent ions (Al^{3+}) displayed *two* competing effects on the equilibrium swelling ratio of PANa-PAM hydrogels: (1) network chain retraction, due to the formation of ionic crosslinks within the network, resulting in the release of fluid; (2) hindered fluid transport, due to the high density of ionic crosslinks that can form in the outer regions of the sample, resulting in a stiff surface shell. For low-concentration PANa samples immersed in Al^{3+} solutions, effect (1) was dominant and the equilibrium swelling ratio decreased. For high-concentration PANa samples immersed in Al^{3+} solutions, effect (2) was dominant and the equilibrium swelling ratio increased. This result indicated that in addition to the valency of ions contained in the swelling fluid, the swelling performance and

fluid release rate of the PANa-PAM hydrogel samples was strongly dependent on the concentration of anionic groups within the polymer network which contribute in ionic crosslinking reactions.

The effect of ion valency on fluid release rate was further verified by the transient swelling response of the PANa-PAM hydrogel sample. The transient swelling response of the 17 wt.% PANa-PAM hydrogel sample immersed in Ca^{2+} did not contain a short-time peak but did display a broad peak when immersed in the Al^{3+} solution (indicating fluid absorption and subsequent release). This was because the ionic crosslinks formed by Al^{3+} were localized in the polymer network compared with the weak and delocalized crosslinks formed by Ca^{2+} and thus the chain retraction forces from the presence of Al^{3+} would be stronger and dominant. This results in fluid release and formation of the broad peak in the transient swelling response. By comparison, the short-time peak for samples containing 67 wt.% PANa immersed in Al^{3+} solutions was very narrow and smaller in magnitude because of hindered fluid transport due to formation of the stiff outer shell which slowed/prevented fluid release. The stronger ionic crosslinks formed by Al^{3+} is the reason for the increased equilibrium swelling ratios for 67 wt.% and 83 wt.% PANa hydrogel samples immersed in Al^{3+} solution compared with samples in Ca^{2+} solution (refer back to Table 1).

Referring back to Figure 6, the short-time swelling peak for samples immersed in Ca^{2+} solutions became narrower as PANa concentration increased. As the amount of ionic crosslinks increased with PANa concentration, the hydrogel samples with greater PANa concentration have an increased tendency to release fluid due to enhanced chain retraction forces which leads to a narrower short-time swelling peak.

3.5 Mechanical Testing of Macroscale PANa-PAM Hydrogel Samples

To further investigate the properties of the macroscale PANa-PAM hydrogel samples, compression tests were performed on macroscale samples swollen in different ionic solutions. Figure 11 displays the compressive stress responses for macroscale hydrogel samples with specific swelling ratios in Ca^{2+} solutions. The calculated elastic moduli of the samples are reported in Table 2. The elastic modulus for the samples with 2 wt.% covalent crosslinking density were much larger than the samples with 1 wt.% density, consistent with rubber elasticity theory (Eq. 2). As shown in Table 2, elasticity was observed to decrease as the swelling ratio increased for the samples with 1 wt.% covalent crosslinking densities while the elasticity of samples containing 2 wt.% covalent crosslinking

density appeared to increase with swelling for the two ratio values investigated here. Figure 11 also displays the almost completely overlapping stress responses of the 2 wt.% covalent crosslinking density samples immersed in water and Ca^{2+} solution with identical swelling ratios of ~ 4.3 g/g.

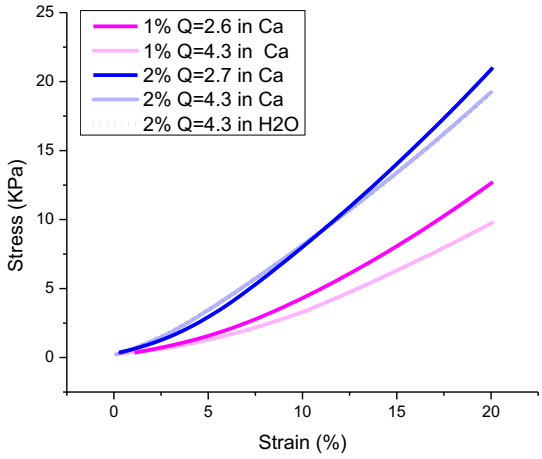

Figure 11. Compressive stress response of macroscale hydrogel samples with 67 wt.% PANa containing 1 or 2 wt.% covalent crosslinking densities and swollen to different Q-ratios in Ca^{2+} and deionized solutions.

Table 2. Elastic moduli of macroscale PANa-PAM hydrogel samples with 67 wt.% PANa containing 1 or 2 wt.% covalent crosslinking density.

Covalent Crosslinking Density	Swelling Ratio, Q (g/g)	Elastic Modulus (Ca^{2+} solutions)
1 wt.%	2.6	26.4 KPa
	4.3	14.8 KPa
2 wt.%	2.7	40.5 KPa
	4.3	54.4 KPa

Figure 12 displays the compressive stress responses for macroscale hydrogel samples containing 67 wt.% PANa and 2 wt.% covalent crosslinking density and swelling ratios of around 2.7 g/g in Al^{3+} and Ca^{2+} solutions. The hydrogel sample displayed a much stiffer stress response following immersion in Al^{3+} solutions than the sample immersed in the Ca^{2+} solutions. Additionally, cracking sounds were heard during compression testing of samples in Al^{3+} solutions. The elastic modulus of the sample

immersed in Al^{3+} solution was calculated to be 102.6 KPa, an order of magnitude larger than results obtained for a similar sample immersed in Ca^{2+} solution (40.5 KPa, see Table 2).

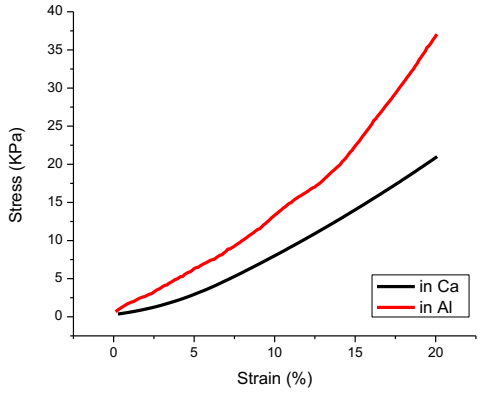

Figure 12. Compressive stress response of macroscale hydrogel samples containing 67 wt.% PANa and 2 wt.% covalent crosslinking density, with swelling ratio of approximately 2.7 g/g in Al^{3+} solutions.

To better understand the mechanical properties of the macroscale hydrogel samples swollen in Al^{3+}, specimens of the stiff outer shell of the hydrogel sample were isolated and tested in tension. Figure 13 displays the tension stress response of the shell specimens after the hydrogel samples reached swelling equilibrium in Al^{3+} solutions. The elastic modulus was calculated to be 59.5 MPa (67 wt.% PANa sample with 1 wt.% covalent crosslinking density), 107.2 MPa (83 wt.% PANa sample with 1 wt.% covalent crosslinking density) and 125.4 MPa (83 wt.% PANa sample with 2 wt.% covalent crosslinking density). Thus, compared to results in Table 2, the elastic modulus for the stiff outer shells of the PANa-PAM hydrogel samples was approximately 1000 times greater than the overall compression modulus of the core-shell samples and the modulus of similar samples immersed in Ca^{2+} solutions.

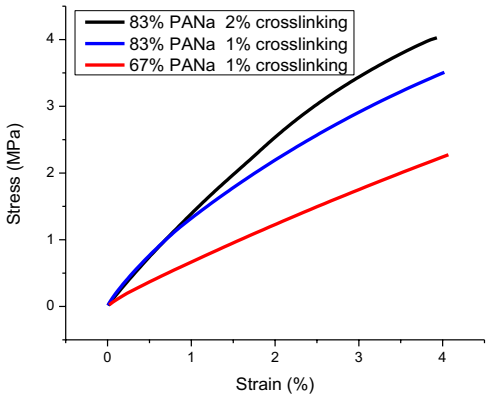

Figure 13. Tensile stress response of specimens of the stiff outer shell of different PANa-PAM hydrogel samples after swelling equilibrium was reached in Al^{3+} solutions.

Discussion

As mentioned in Section 3.2, the ionic crosslinks formed by Ca^{2+} ions are relatively weak and delocalized within the network and prior work has found that the aggregation of polymer chains caused by Ca^{2+} ions doesn't affect the elastic modulus of polymer network.(Horkay et al. 2000) This explained why the compressive stress responses of the 2 wt.% covalent crosslinking density samples immersed in water and Ca^{2+} solution almost perfectly overlap with each other (shown in Figure 11). Also stated in Section 3.3, increased covalent crosslinking density leads to increased elastic modulus (*i.e.*, rubber elasticity theory)(Rubinstein and Colby 2003) which provides rationale for effective doubling of the elastic modulus in Table 2 when the covalent crosslinking density increased from 1 wt.% to 2 wt.% for PANa-PAM hydrogel samples with 67 wt.% PANa immersed in Ca^{2+} solutions. It was also observed that the equilibrium swelling ratio affected the compressive stress response of PANa-PAM hydrogels immersed in Ca^{2+} solutions, with greater swelling ratios resulting in reduced elastic moduli. The greater volume of water within the hydrogel allows for increased segmental mobility of the polymer chains in the network and subsequently faster relaxation in response to an applied stress. This was confirmed by the reduced elastic modulus of samples with 1 wt.% covalent crosslinking densities (Table 2). However, the opposite trend was observed for samples with 2 wt.% covalent crosslinking densities. This could be due to an imperfection of the particular sample or it is

equally likely that for the range of swelling ratios investigated here, the elastic modulus is more strongly dependent the covalent density and more weakly dependent on swelling ratio.

The cracking sound that was observed during mechanical testing of samples swollen in Al^{3+} solutions suggested that the stiff outer shell (seen in Figure 10b) was very hard and brittle. This stiff shell resulted in the overall stiffer mechanical response that was observed during compression testing of samples equilibrated in Al^{3+} solutions compared with the response of samples equilibrated in Ca^{2+} solutions (see Figure 12). The isolated tensile stress response of specimens of the PANa-PAM hydrogel's outer shell layer further explains the nature of the strong ionic crosslinks formed by Al^{3+}. The elastic modulus of the stiff shells was observed to be in the MPa range. As shown in Figure 13, increased PANa concentration in the hydrogel sample strongly enhanced the shell's stiffness, most likely due to increased density of the Al^{3+} ionic crosslinks in the outer region of the sample facilitated by the greater overall concentration of anionic groups in the polymer network of the high-concentration PANa hydrogel samples. By comparison, only weak enhancement of the shell's stiffness was observed with an increase in covalent crosslinking density from 1 wt.% to 2 wt.% (Figure 13). Thus, the enhanced mechanical properties of the PANa-PAM hydrogel samples were primarily a result of the presence of Al^{3+} and the subsequent formation of a strong, ionically crosslinked, core-shell structure.

4.0 Summary and Main Conclusions

The effect of ions on the swelling and mechanical properties of model SAP hydrogels was characterized here, using a series of poly(sodium acrylate-acrylamide) (PANa-PAM) random copolymer networks with varying concentrations of PANa. By synthesizing the hydrogels in-house, samples with independently tunable amounts of covalent crosslinking and anionic functional groups were created, allowing for the effects of covalent and ionic crosslinking on the properties of the hydrogels to be separately quantified. Free swelling experiments were performed with PANa-PAM hydrogel samples with three particle sizes (106-425 μm, 425-850 μm, and mm-sized "macroscale" samples). For the experiments, the swelling capacity and kinetics were characterized during sample immersion in deionized water and Na^{+}, Ca^{2+}, and Al^{3+} solutions. Mechanical tests were also performed

on the macroscale samples following equilibration in the different solutions. The main experimental outcomes were the following:

- The swelling capacity and kinetics of PANa-PAM hydrogels was strongly sensitive to the presence of ions in solution. For hydrogel samples containing a relatively low concentration of PANa (17, 33 wt.%), the equilibrium swelling ratio decreased in the following fashion: Q(water) > $Q(Na^+)$ > $Q(Ca^{2+})$ > $Q(Al^{3+})$. For hydrogel samples containing a relatively high concentration of PANa (67, 83 wt.%), the equilibrium swelling ratio decreased in the following fashion: Q(water) > $Q(Na^+)$ > $Q(Al^{3+})$ > $Q(Ca^{2+})$. The presence of ions caused rapid swelling and de-swelling of the samples to occur.
- Increased covalent crosslinking density in the PANa-PAM hydrogel samples resulted in a decreased equilibrium swelling ratio for samples immersed in water or Na^+ solutions, consistent with theories from rubber elasticity. However in the presence of ions, the swelling performance of the hydrogels became less sensitive to covalent crosslinking density.
- Compression testing of samples immersed in Ca^{2+} solutions indicated that greater swelling ratio or reduced covalent crosslinking density resulted in hydrogels with reduced elastic modulus (~ kPa), again consistent with rubber elasticity theories. More importantly, the stress response of samples immersed in Ca^{2+} was found to be almost identical to the response of samples immersed in pure water at equivalent Q-values, indicating that the ionic crosslinks formed by Ca^{2+} ions had no significant impact on the mechanical properties of the samples.
- For hydrogel samples with high PANa concentration (67 wt.% or 83 wt.%), formation of a mechanically stiff layer at the hydrogel's surface was observed during immersion in Al^{3+} solutions. This stiff "shell" displayed elastic moduli of O(100 MPa), which caused the overall elastic modulus of the hydrogel to increase and also prevented the release of fluid from the hydrogel. This effect was not observed during immersion in the Ca^{2+} solutions.

Overall, the swelling performance, swelling kinetics, and mechanical properties of PANa-PAM hydrogels were found to be strongly dependent on the concentration of anionic groups in the polymer network and the valency of the ions in the swelling media. The results described here have the following implications. First, by informed selection of the concentration of anionic groups within the polymer network of a SAP particle, it is possible to control the maximum swelling ratio and initial swelling rate, which could be used to create customized SAP particles designed for specific cementing

environments. Second, the results presented here may be useful for the development of predictive models that capture the behavior of SAP particles in cement. With only prior knowledge of the expected concentration and valency of ions in the pore fluid, such models would allow for quantitative predictions of the concentration of anionic groups in the polymer network that would be required to create SAP particles with a desired swelling capacity, fluid release rate, and mechanical response.

ACKNOWLEDGEMENTS

The authors thank Prof. W. Jason Weiss and graduate student Timothy Barrett in the School of Civil Engineering at Purdue University for helpful discussions during the course of the project.

REFERENCES

Andersson K, Allard B, Bengtsson M, Magnusson B (1989) Chemical composition of cement pore solutions. Cement and Concrete Research 19:327–332. doi: 10.1016/0008-8846(89)90022-7

Bahaj H, Benaddi R, Bakass M, Bayane C (2010) Swelling of Superabsorbents Polymers in an Aqueous Medium. Journal of Applied Polymer Science 115:2479–2484. doi: 10.1002/app

Di Bella C, Schlitter J, Carboouneau N, Weiss WJ (2012a) Documenting the Construction of a Plain Concrete Bridge Deck and an Internally Cured Bridge Deck - Joint Transportation Research Program.

Di Bella C, Villani C, Phares N, et al. (2012b) Chloride Transport and Service Life in Internally Cured Concrete. American Society of Civil Engineers Structures Congress

Bentur A, Igarashi S, Kovler K (2001) Prevention of autogenous shrinkage in high-strength concrete by internal curing using wet lightweight aggregates. Cement and Concrete Research 31:1587–1591. doi: 10.1016/S0008-8846(01)00608-1

Bentz D, Halleck P (2006) Water movement during internal curing: Direct observation using x-ray microtomography. Concrete Internaltional 28:39–45.

Breitenbiicher R (1998) Developments and applications of high-performance concrete. Materials and Structures 31:209–215.

Buchholz FL (1994) Preparation Methods of Superabsorbent Polyacrylates. Superabsorbent Polymers. pp 27–38

Buchholz FL (1998) Absorbency and superabsorbency. In: Buchholz FL, Graham AT (eds) Modern superabsorbent polymer technology. John Wiley & Sons, pp 1–18

Chen X-P, Shan G-R, Huang J, et al. (2004) Synthesis and properties of acrylic-based superabsorbent. Journal of Applied Polymer Science 92:619–624. doi: 10.1002/app.20052

Chen Z, Liu M, Ma S (2005) Synthesis and modification of salt-resistant superabsorbent polymers. Reactive and Functional Polymers 62:85–92. doi: 10.1016/j.reactfunctpolym.2004.09.003

Cusson D, Hoogeveen T (2008) Internal curing of high-performance concrete with pre-soaked fine lightweight aggregate for prevention of autogenous shrinkage cracking. Cement and Concrete Research 38:757–765. doi: 10.1016/j.cemconres.2008.02.001

Double DD, Hewlett PC, Sing KSW, Raffle JF (1983) New Developments in Understanding the Chemistry of Cement Hydration [and Discussion]. Philosophical Transactions of the Royal Society A: Mathematical, Physical and Engineering Sciences 310:53–66. doi: 10.1098/rsta.1983.0065

Esteves LP (2011) Superabsorbent polymers: On their interaction with water and pore fluid. Cement and Concrete Composites 33:717–724. doi: 10.1016/j.cemconcomp.2011.04.006

Gary D. Christian (2004) Analytical Chemistry. 742–744.

Geiker MR, Bentz DP, Jensen OM (2004) Mitigating Autogeneous Shrinkage by Internal Curing Mitigating Autogenous Shrinkage by Internal Curing. High-Performance Structural Lightweight Concrete. pp 143–148

Guthrie WS, Yaede JM (2013) Internal Curing of Concrete Bridge Decks in Utah: Preliminary Evaluation - Transportation Research Board. 17.

Hasholt MT, Jensen OM, Kovler K, Zhutovsky S (2012) Can superabsorent polymers mitigate autogenous shrinkage of internally cured concrete without compromising the strength? Construction and Building Materials 31:226–230. doi: 10.1016/j.conbuildmat.2011.12.062

Henderson KJ, Zhou TC, Otim KJ, Shull KR (2010) Ionically Cross-Linked Triblock Copolymer Hydrogels with High Strength. Macromolecules 43:6193–6201. doi: 10.1021/ma100963m

Horkay F, Tasaki I, Basser PJ (2000) Osmotic swelling of polyacrylate hydrogels in physiological salt solutions. Biomacromolecules 1:84–90.

Horkay F, Tasaki I, Basser PJ (2001) Effect of monovalent-divalent cation exchange on the swelling of polyacrylate hydrogels in physiological salt solutions. Biomacromolecules 2:195–9.

Jar P-YB, Wu YS (1997) Effect of counter-ions on swelling and shrinkage of polyacrylamide-based ionic gels. Polymer 38:2557–2560. doi: 10.1016/S0032-3861(97)01023-9

Jensen OM, Hansen PF (2001) Water-entrained cement-based materials I . Principles and theoretical background. Cement and Concrete Research 31:647–654.

Jensen OM, Hansen PF (2002) Water-entrained cement-based materials II. Experimental observations. Cement and Concrete Research 32:973–978. doi: 10.1016/S0008-8846(02)00737-8

Jones W (2013) “Freeze-Thaw Behavior of Internally Cured Concrete”. Purdue University

Kovler K, Jensen O (2007) RILEM Report 41 Internal Curing of Concrete – State of the Art Report of TC 1966-IC. 140.

Lura P, Friedemann K, Stallmach F, et al. (2012) Kinetics of Water Migration in Cement-Based Systems Containing Superabsobent Polymers. Application of Super Absorbent Polymers (SAP) in Concrete Construction. Springer Netherlands, pp 21–37

Lura P, Jensen O, Breugel K van (2003) Autogenous shrinkage in high-performance cement paste: An evaluation of basic mechanisms. Cement and Concrete Research 33:223–232.

Murali Mohan Y, Keshava Murthy PS, Mohana Raju K (2006) Preparation and swelling behavior of macroporous poly(acrylamide-co-sodium methacrylate) superabsorbent hydrogels. Journal of Applied Polymer Science 101:3202–3214. doi: 10.1002/app.23277

Raju KM, Raju MP, Mohan YM (2003) Synthesis of superabsorbent copolymers as water manageable materials. Polymer International 52:768–772. doi: 10.1002/pi.1145

Reinhardt HW, Assman A, Monning S (2008) Superabsorbent polymers (SAP) – An Admixture to Increase the Durability of Concrete. In: Sun W, van Breugel K, Miao C, et al. (eds) International Conference on Microstructure Related Durability of Cementitious Composites. pp 313–322

Rubinstein M, Colby RH (2003) Polymer Physics. OUP Oxford

Schlitter J, Henkensiefken R, Castro J, et al. (2010) Development of Internally Cured Concrete for Increased Service Life - FHWA/IN/JTRP-2010/10.

Schlitter JL, Bentz DP, Weiss WJ (2013) Quantifying Residual Stress Development and Reserve Strength in Internally Cured Concrete. American Concrete Institute Journal of Materials

Schröfl C, Mechtcherine V, Gorges M (2012) Relation between the molecular structure and the efficiency of superabsorbent polymers (SAP) as concrete admixture to mitigate autogenous shrinkage. Cement and Concrete Research 42:865–873. doi: 10.1016/j.cemconres.2012.03.011

Siramanont J, Vichit-Vadakan W, Siriwatwechakul W (2010) The impact of SAP structure on the effectiveness of internal curing. In: Jensen OM, Hasholt MT, Laustsen S (eds) International RILEM conference on Use of superabsorbent polymers and other new additives in concrete. RILEM, Lyngby, Denmark, pp 243–252

Siriwatwechakul W, Siramanont J, Vichit-Vadakan W (2012) Behavior of Superabsorbent Polymers in Calcium- and Sodium-Rich Solutions. Journal of Materials in Civil Engineering 24:976–980. doi: 10.1061/(ASCE)MT.1943-5533.0000449

Siriwatwechakul W, Siramanont J, Vichit-Vadakan W (2010) Superabsorbent polymer structures. In: Jensen OM, Hasholt MT, Laustsen S (eds) International RILEM conference on Use of superabsorbent polymers and other new additives in concrete. RILEM, Lyngby, Denmark, pp 253–263

Snoeck D, Tittelboom K V., Steuperaert S, et al. (2012) Self-healing cementitous materials by the combination of microfibers and superabsorbent polymers. Journal of Intelligent Material Systems and Structures 12.

Staples TL, Henton DE, Buchholz FL (1998) Chemistry of superabsorbent polyacrylates. In: Buchholz FL, Graham AT (eds) Modern superabsorbent polymer technology. John Wiley & Sons, pp 19–68

Streeter DA, Wolfe WH, Vaughn RE (2012) Field Performance of Internally Cured Concrete Bridge Decks in New York State. ACI SP 290

Weiss WJ, Yang W, Shah SP (1998) Shrinkage Cracking of Restrained Concrete Slabs. Journal of Engineering Mechanics 124:765–774. doi: 10.1061/(ASCE)0733-9399(1998)124:7(765)

Wyrzykowski M, Lura P (2013) Controlling the coefficient of thermal expansion of cementitious materials – A new application for superabsorbent polymers. Cement and Concrete Composites 35:49–58. doi: 10.1016/j.cemconcomp.2012.08.010

Yarimkaya S, Basan H (2007) Synthesis and Swelling Behavior of Acrylate-Based Hydrogels. Journal of Macromolecular Science, Part A 44:699–706. doi: 10.1080/10601320701351268

Zhang Y, Wang L, Li X, He P (2010) Salt-resistant superabsorbents from inverse-suspension polymerization of PEG methacrylate, acryamide and partially neutralized acrylic acid. Journal of Polymer Research 18:157–161. doi: 10.1007/s10965-010-9402-8